AMERICAN SOCIETY FOR MICROBIOLOGY | Applied and Environmental Microbiology®

GENETICS AND MOLECULAR BIOLOGY

The Cell Wall Integrity Pathway Contributes to the Early Stages of *Aspergillus fumigatus* Asexual Development

Marina Campos Rocha,[a] João Henrique Tadini Marilhano Fabri,[a] Isabelle Taira Simões,[a] Rafael Silva-Rocha,[b] Daisuke Hagiwara,[c] Anderson Ferreira da Cunha,[a] Gustavo Henrique Goldman,[d] David Cánovas,[e] Iran Malavazi[a]

[a]Departamento de Genética e Evolução, Centro de Ciências Biológicas e da Saúde, Universidade Federal de São Carlos, São Carlos, São Paulo, Brazil
[b]Departamento de Biologia Celular e Molecular, Faculdade de Medicina de Ribeirão Preto, Universidade de São Paulo, Ribeirão Preto, São Paulo, Brazil
[c]Faculty of Life and Environmental Sciences, University of Tsukuba, Ibaraki, Japan
[d]Departamento de Ciências Farmacêuticas, Faculdade de Ciências Farmacêuticas de Ribeirão Preto, Universidade de São Paulo, Ribeirão Preto, São Paulo, Brazil
[e]Department of Genetics, University of Seville, Seville, Spain

ABSTRACT *Aspergillus fumigatus* is a major cause of human disease. The survival of this fungus is dependent on the cell wall organization and function of its components. The cell wall integrity pathway (CWIP) is the primary signaling cascade that controls *de novo* synthesis of the cell wall in fungi. Abundant conidiation is a hallmark in *A. fumigatus*, and uptake of conidia by a susceptible host is usually the initial event in infection. The formation of conidia is mediated by the development of fungus-specific specialized structures, conidiophores, which are accompanied by cell wall remodeling. The molecular regulation of these changes in cell wall composition required for the rise of conidiophore from the solid surface and to disperse the conidia into the air is currently unknown. Here, we investigated the role of CWIP in conidiation. We show that CWIP *pkcA*^{G579R}, Δ*mpkA*, and Δ*rlmA* mutants displayed reduced conidiation during synchronized asexual differentiation. The transcription factor RlmA directly regulated the expression of regulators of conidiation, including *flbB*, *flbC*, *brlA*, *abaA*, and *rasB*, as well as genes involved in cell wall synthesis and remodeling, and this affected the chitin content in aerial hyphae. Phosphorylation of RlmA and MpkA was increased during asexual differentiation. We also observed that MpkA physically associated with the proteins FlbB, FlbC, BrlA, and RasB during this process, suggesting another level of cross talk between the CWIP and asexual development pathways. In summary, our results support the conclusion that one function of the CWIP is the regulation of asexual development in filamentous fungi.

IMPORTANCE A remarkable feature of the human pathogen *Aspergillus fumigatus* is its ability to produce impressive amounts of infectious propagules known as conidia. These particles reach immunocompromised patients and may initiate a life-threatening mycosis. The conidiation process in *Aspergillus* is governed by a sequence of proteins that coordinate the development of conidiophores. This process requires the remodeling of the cell wall so that the conidiophores can rise and withstand the chains of conidia. The events regulating cell wall remodeling during conidiation are currently unknown. Here, we show that the cell wall integrity pathway (CWIP) components RlmA and MpkA directly contribute to the activation of the conidiation cascade by enabling transcription or phosphorylation of critical proteins involved in asexual development. This study points to an essential role for the CWIP during conidiation and provides further insights into the complex regulation of asexual development in filamentous fungi.

KEYWORDS asexual development, *Aspergillus fumigatus*, cell wall integrity, MpkA, PkcA, RlmA

Citation Rocha MC, Fabri JHTM, Simões IT, Silva-Rocha R, Hagiwara D, da Cunha AF, Goldman GH, Cánovas D, Malavazi I. 2020. The cell wall integrity pathway contributes to the early stages of *Aspergillus fumigatus* asexual development. Appl Environ Microbiol 86:e02347-19. https://doi.org/10.1128/AEM.02347-19.

Editor Irina S. Druzhinina, Nanjing Agricultural University

Address correspondence to Iran Malavazi, imalavazi@ufscar.br.

Received 14 October 2019
Accepted 10 January 2020
Accepted manuscript posted online 31 January 2020
Published 18 March 2020

The filamentous fungus *Aspergillus fumigatus* is the leading causative agent of invasive pulmonary aspergillosis, a severe systemic infection with high mortality rates in the immunocompromised population (1, 2). Asexual spores (conidia) are infectious propagules of *A. fumigatus* and are dispersed through the air and water via their displacement from fungal aerial structures (3). Other features of the conidia, such as small size and high hydrophobicity, are well-established virulence determinants for this pathogen (3–5). Infection usually occurs through the inhalation of conidia by the host, which subsequently germinate into hyphae and form a mycelium within the lung tissue (6, 7).

Fungal cell survival in the host and environment is highly dependent on the function, organization, and composition of the cell wall. In addition to providing structural integrity to the cells, this dynamic structure also stands out as the main line of fungal defense against the environment (8). The cell wall undergoes constant biosynthesis and remodeling due to natural processes that support fungal growth and reproduction or environmental stress responses (9). The biosynthesis and maintenance of the cell wall are controlled by the cell wall integrity pathway (CWIP), which is a conserved signaling transduction cascade that maintains cell wall homeostasis in fungi (10). Deficiencies in the proteins involved in this signaling cascade in *A. fumigatus* cause virulence attenuation and increased sensitivity to antifungal agents (11–16). The CWIP of *A. fumigatus* requires the activation of the apical kinase PkcA, which occurs via the function of upstream components (13, 14). PkcA activates the three-component mitogen-activated protein kinases (MAPKs) through the phosphorylation of Bck1, which then activates the downstream kinase Mkk2 and finally MpkA (11, 12). MpkA therefore controls the activity of the RlmA transcription factor, which is responsible for regulating the expression of genes related to cell wall biosynthesis (16).

The composition and organization of the cell wall varies according to the fungal morphotypes. Although structural molecules, such as β-(1,3)-glucan, α-(1,3)-glucan, galactomannan, and chitin, are present in the cell walls of both conidia and hyphae, others can be found only in one morphotype. For instance, galactosaminogalactan is found exclusively in hyphae, while the melanin pigment and the hydrophobic rodlet proteins are enriched in conidia cell walls (8, 9). Despite these differences in the cell wall between these morphotypes, the changes occurring in the cell wall during asexual development and the role played by CWIP during this process are unknown.

Aspergillus asexual reproduction has been largely studied, and pivotal information about this process is available (17–20). The entire process is genetically regulated by upstream developmental activators (UDAs) and negative repressors, the central regulatory pathway (CRP), and light-responsive and velvet regulators (17–26). Six UDAs control the initiation of the conidial developmental pathway in *A. fumigatus*: *fluG*, *flbA*, *flbB, flbD, flbE*, and *flbC* (24, 26). Activation of the CRP is thus a consequence of the expression of UDA genes. The CRP module contains three essential genes, *brlA*, *abaA*, and *wetA* (23), which are sequentially responsible for coordinating conidiation and gene-specific expression during this process (reviewed in references 18 to 20 and 27). BrlA is a crucial activator for the initiation of development in *Aspergillus*, which is required for proper expression of genes related to conidiation, such as *abaA* and *wetA*, and for the transition between vesicles and metulae (22, 25). AbaA is also a transcription activator and a key regulator for conidiophore morphology and phialide formation, while *wetA* is essential for the final steps of conidiation and conidial cell wall formation (25, 28).

The involvement of the CWIP in conidiogenesis has been previously reported deduced based on the impaired conidiation phenotype observed for the Δ*mpkA* and Δ*rlmA* strains in radial colonies (12, 16, 29). However, the molecular interplay between the CWI and conidiation pathways has not been established. Here, we observe that the CWIP is induced both at the protein and transcriptional levels during asexual development, and the loss-of-function of CWIP components results in impaired conidiation in synchronized cultures. We observe that the RlmA transcription factor directly binds to the promoters of key conidiation regulators, including *flbB*, *flbC*, *brlA*, and *rasB*, as

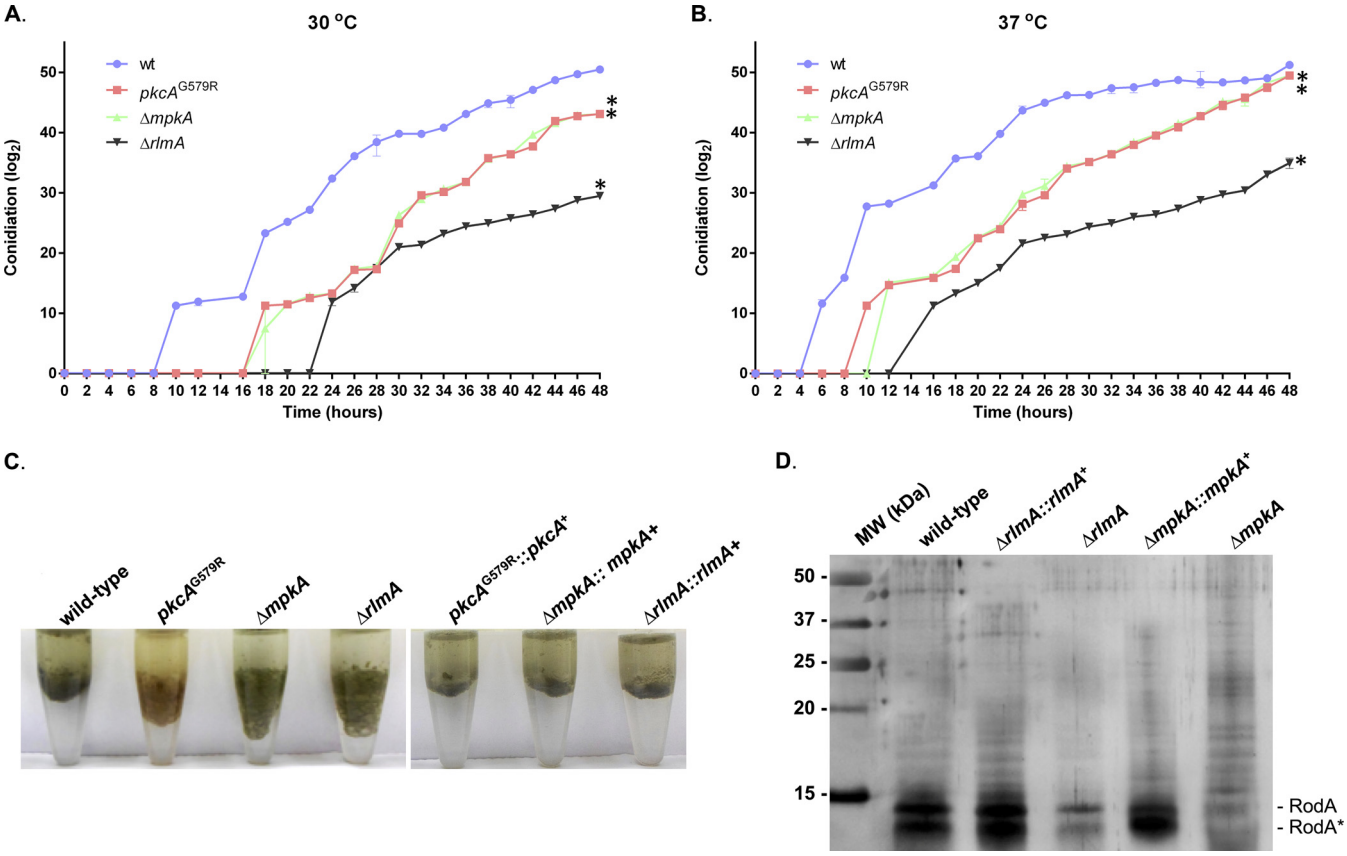

FIG 1 The CWIP mutants have delayed conidiation when asexual differentiation is induced and altered hydrophobicity of conidia. Conidia were counted by sampling the mycelium of each strain subjected to synchronized asexual differentiation at 2-h intervals at 30°C (A) and 37°C (B). The results are the averages ± the standard deviations (SD; $n = 3$; *, $P \leq 0.01$ for all time points). Absolute values of quantification were $\log_2$ transformed and raw data are available in Data Set S1. (C) Altered hydrophobic properties of conidia in a 1:1 water-oil (tributyrin) interface. (D) Silver-stained SDS-PAGE showing the hydrophobin content extracted from resting conidia. RodA corresponds to the native RodA, and RodA* corresponds to partially degraded or processed RodA (according to reference 50).

well as cell wall remodeling genes, such as chitinases and glucanases, regulating their expression. In addition, we observe that concomitant protein-protein interactions occur between the MAPK MpkA and these conidiation regulatory proteins.

RESULTS

The CWIP mutants exhibit reduced conidiation. Following our phenotypic examinations of the Δ*rlmA* strain (16), we noticed that this strain displayed reduced conidiation and a fluffy-like phenotype in both complete and minimum media; this was represented by the formation of seemingly undifferentiated aerial hyphae, which were more evident at 30°C, suggesting that *rlmA* is necessary for normal levels of conidiation (see Fig. S1 in the supplemental material).

Subsequently, we decided to evaluate in more detail the conidiation defect of the Δ*rlmA* mutant and the main upstream components of the CWIP, *pkcA* and *mpkA*, upon synchronized asexual differentiation, at both 30 and 37°C (Fig. S2). We monitored conidia production up to 48 h after the beginning of the asexual conidiation and the results indicated a noticeable delay in the formation of conidia in the mycelia of the Δ*rlmA* mutant at both temperatures. We observed that the *pkcA*^{G579R} and Δ*mpkA* strains also exhibited the same phenotype, suggesting that the PkcA-MpkA-RlmA circuit is necessary for the timing of conidiation (Fig. 1A and B; Fig. S2). Notably, the delay in conidiogenesis observed for the Δ*rlmA* mutant was more severe than that displayed by the other mutants, even though the Δ*mpkA* strain has the most reduced radial growth (12). For instance, the wild-type strain produced conidia after 10 h (30°C)

or 6 h (37°C), whereas in the Δ*rlmA* mutant, conidia were initially detected only after 24 h (30°C) or 16 h (37°C). Despite this marked defect in conidiation, no abnormalities in the conidiophore structures of the Δ*rlmA* mutant were observed (Fig. S3). So, this observation is likely a function of delayed onset of asexual development rather than the rate of conidial production. Likewise, the *pkcA*^{G579R} and Δ*mpkA* strains were able to form normal conidiophores, as previously reported (11, 15).

Other factors, such as the hydrophobins, especially the RodA protein, which is covalently bound to the conidial cell wall through glycosylphosphatidylinositol-remnants, can play a role in asexual development, e.g., by allowing aerial structures to move into the air. Since alterations in the composition of the cell wall have been reported in the *pkcA* and *rlmA* strains (11, 16), we investigated the hydrophobic properties of the conidia and the content of surface hydrophobin in these mutants. For all mutants, conidia showed a drastic alteration in hydrophobicity, and again, this phenotype was more evident in the Δ*rlmA* mutant. In addition, the RodA content was highly reduced in the Δ*rlmA* and Δ*mpkA* strains (Fig. 1C and D). The lower accumulation of RodA in the *pkcA*^{G579R} was previously reported (11).

The expression of *pkcA* and *rlmA* and the phosphorylation of MpkA are induced during synchronized asexual development in *A. fumigatus*. Based on the aforementioned phenotypes, we hypothesized that the initial regulatory events of asexual development require the function of CWIP. Next, we examined the expression of *pkcA*, *mpkA*, and *rlmA* during conidiation. Interestingly, an increase in the mRNA accumulation of *pkcA* and *rlmA* in the wild-type strain during asexual development at 30 and 37°C was observed, suggesting that transcriptional upregulation of CWIP is linked to conidiation events (Fig. S4). However, we observed a decrease in *mpkA* mRNA abundance during the developmental asexual induction, at both 30 and 37°C (Fig. S4). Notably, *rlmA* mRNA levels were induced at least 4-fold at both 30 and 37°C after the submerged cultures were transferred to the solid surface-air interface. *pkcA* mRNA levels were significantly reduced at both temperatures in the Δ*rlmA* deletion compared to the wild type. Consistently, *mpkA* mRNA levels were also lower in the Δ*rlmA* mutant but only at 30°C, when the fluffy-like phenotype was more evident (Fig. S1).

To confirm the activation of CWIP during asexual development, MpkA phosphorylation was assessed by Western blotting in the wild-type, *pkcA*^{G579R} and Δ*rlmA* strains. Despite lower *mpkA* mRNA abundance, increased MpkA phosphorylation was observed in the wild-type strain at both temperatures peaking after 36 h at 30°C and after 12 h at 37°C (Fig. 2A and B). In contrast, MpkA phosphorylation was maintained at lower and constant levels in the *pkcA*^{G579R} mutant, whereas it was almost absent in the Δ*rlmA* mutant. To determine whether RlmA activation also occurs during conidiation, we investigated the phosphorylation state of RlmA in wild-type cells containing a C-terminal RlmA::3×FLAG epitope. Phosphorylated RlmA was abundantly observed 6 to 24 h postinduction of conidiation at 37°C, while the unphosphorylated form of the protein predominated in the hyphal state. Consistently, the bands indicating slower migrating forms of RlmA disappeared when protein extracts were treated with calf intestinal alkaline phosphatase (Fig. 2C). This result suggests that multiple phosphorylation sites are present in RlmA and that the observed phosphorylation of this protein is directed by the onset of conidiation and the cell wall composition changes that occur during asexual development. Altogether, the data suggest that the signaling emerging from PkcA-MpkA-RlmA activity contributes to the early steps of conidiation.

Since our data suggest CWIP signaling is activated during asexual development and required for wild-type levels of conidiation, we next investigated whether components of the cell wall changed during this developmental program. As an initial approach to address this question, we used calcofluor white (CFW) as a probe to detect fluctuations in the chitin content of the aerial hyphae over time (30). Our results, surprisingly, indicate that there are no differences between the wild-type and the *pkcA*^{G579R} strains with CFW staining. In contrast, Δ*mpkA* and Δ*rlmA* strains showed reduced or increased CFW signals, respectively, in comparison to the wild-type strain (Fig. S5). This analysis implies that the Δ*mpkA* strain accumulates or exhibits less chitin in the cell wall, while

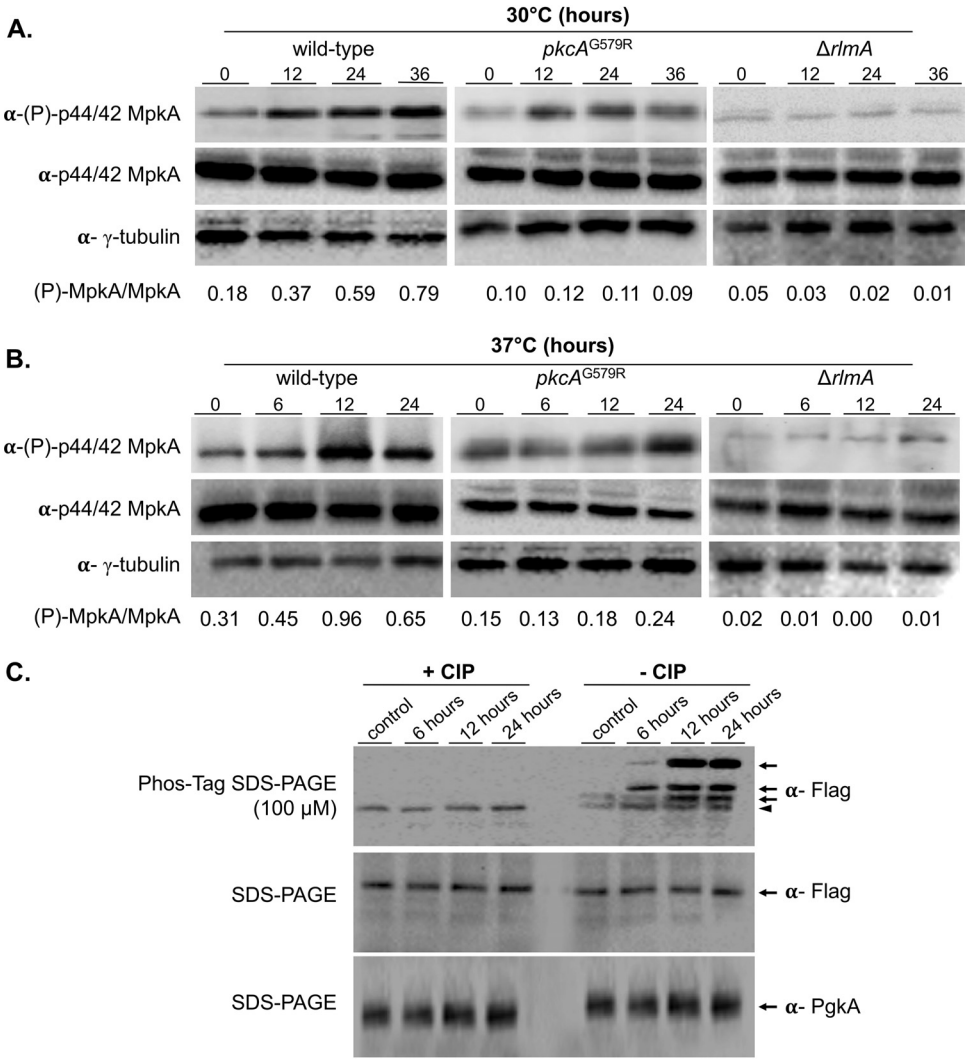

FIG 2 CWIP is activated during asexual development and is accompanied by RlmA phosphorylation. (A and B) Western blotting assay of MpkA phosphorylation in a time course experiment of synchronized asexual differentiation. α-(P)-p44/42 or α-p44/42 antibodies were used to detect the phosphorylation and total MpkA, respectively. α-γ-Tubulin antibody was used as a loading control. Signal intensities were quantified, and the ratios of (P)-MpkA to MpkA were calculated and are shown below the panels. (C) Western blot of protein from the *rlmA*::3×FLAG treated (+ CIP) or not (− CIP) with calf intestinal alkaline phosphatase and probed with α-FLAG antibody in membranes obtained from Phos-tag or regular 8% SDS-PAGE. The arrows point to the phosphorylated forms of RlmA, and the arrowhead points to the unphosphorylated protein. Predicted protein sizes on blot: MpkA, 48.5 kDa; and RlmA::3×FLAG, 70.3 kDa.

the opposite occurs in the Δ*rlmA* strain and suggests that alterations in cell wall composition and organization correlate with the delay in conidiation observed in the CWIP mutants.

mRNA abundance of the central regulators of asexual development is altered upon defective CWIP signaling. We reasoned that the conidiation defects in the CWIP mutants could be due to dysregulated expression of the asexual developmental regulators. To test this hypothesis, we examined the mRNA abundance of the CRP genes *brlA*, *abaA*, and *wetA* in the CWIP mutants and wild-type strain during conidiogenesis. As widely expected, mRNA abundance of all three CRP genes was noticeably induced in the wild-type strain at both temperatures (Fig. 3). In contrast, a strong reduction of mRNA abundance of these genes was observed in all CWIP mutants. Although not completely abrogated, the mRNA abundance of *abaA* and *wetA* reached the lowest values in these mutant strains at both temperatures. The only exception was

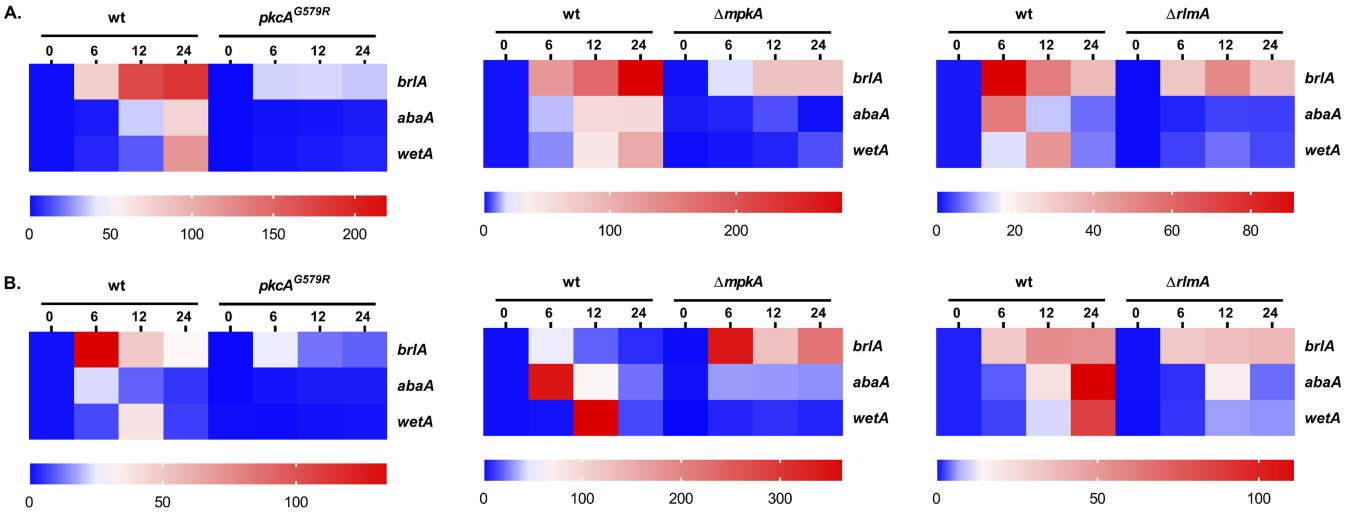

FIG 3 The CWIP mutant strains present lower mRNA abundance of genes encoding the central regulators of asexual development. Expression of *brlA*, *abaA*, and *wetA* was investigated by RT-qPCR in the strains subjected to synchronized asexual differentiation during the indicated time points (hours) at 30°C (A) and 37°C (B). Values represent the averages of the results from three independent experiments with two technical repetitions each (see Fig. S6; $^*P \leq 0.01$ one-way ANOVA), presented as the relative expression of the mutant strain compared to the same time point of the wild-type strain.

observed for *brlA* mRNA abundance (37°C) in the Δ*mpkA* background (Fig. 3B). These results strongly suggest that the CWIP is required for appropriate timing and expression of asexual CRP genes.

Considering the delayed and lower conidiation observed in the Δ*rlmA* strain, we subsequently hypothesized that this transcription factor could play a direct role in the transcriptional activation of the conidiation genes. To address this question, we examined the *A. fumigatus* genome for the predicted RLM box motif at the promoter region of genes encoding regulators of asexual development. The complete list of genes for which the RlmA binding motif was identified is available in Data Set S2. We screened 9841 promoter sequences for the putative MADS-box, and from this data set we were able to identify 1,237 putative sites on the promoters of 544 genes representing 5.5% of the total number of promoters. This search indicated that among the CRP genes, *brlA* and *abaA* but not *wetA* presented putative binding sites for RlmA. In addition, we identified the RlmA binding motif at the promoter regions of two UDAs, i.e., *flbB* and *flbC*, and at the Ras family protein *rasB*, which plays crucial roles in morphogenesis and conidiation (31).

In all these cases, except for the *brlA* and *abaA* promoters, the predicted binding sites corresponding to the 5′-YTAWWWWTAR-3′ motif were present (Fig. 4A). Since the DNA core sequence 5′-TAWWWWTA-3′ was fully conserved in the *brlA* and *abaA* promoters, we decided to include these genes in further analysis because the nucleotides Y (=C or T) or R (=A or G) at the 5′ or 3′ region of the DNA core sequence can differ (29, 32). To examine the binding of RlmA to the promoter region of the conidiation genes, we carried out chromatin immunoprecipitation/quantitative PCR (ChIP-qPCR) experiments using the *rlmA*::GFP strain submitted to synchronized asexual differentiation. The results revealed significant *in vivo* binding of RlmA to the promoter regions of *flbB*, *flbC*, *brlA*, and *abaA* in at least two time points compared to the negative (non-GFP tagged) control strain (Fig. 4B). Notably, binding of RlmA to the promoter of *rasB* was observed only after 24 h of conidiation, which coincides with the putative role of the Ras signaling pathway in morphogenesis and vegetative growth (19).

Based on these observations, we utilized RT-qPCR to analyze the mRNA abundance of *flbB*, *flbC*, and *rasB* in the CWIP mutant strains under the same growth conditions. The results show that *pkcA*, *mpkA*, and *rlmA* are required for the transcription of both *flbB* and *flbC* since the mRNA abundance of both genes is significantly reduced in the CWIP mutants (Fig. 5). Although the promoter region of *rasB* possesses a functional RlmA

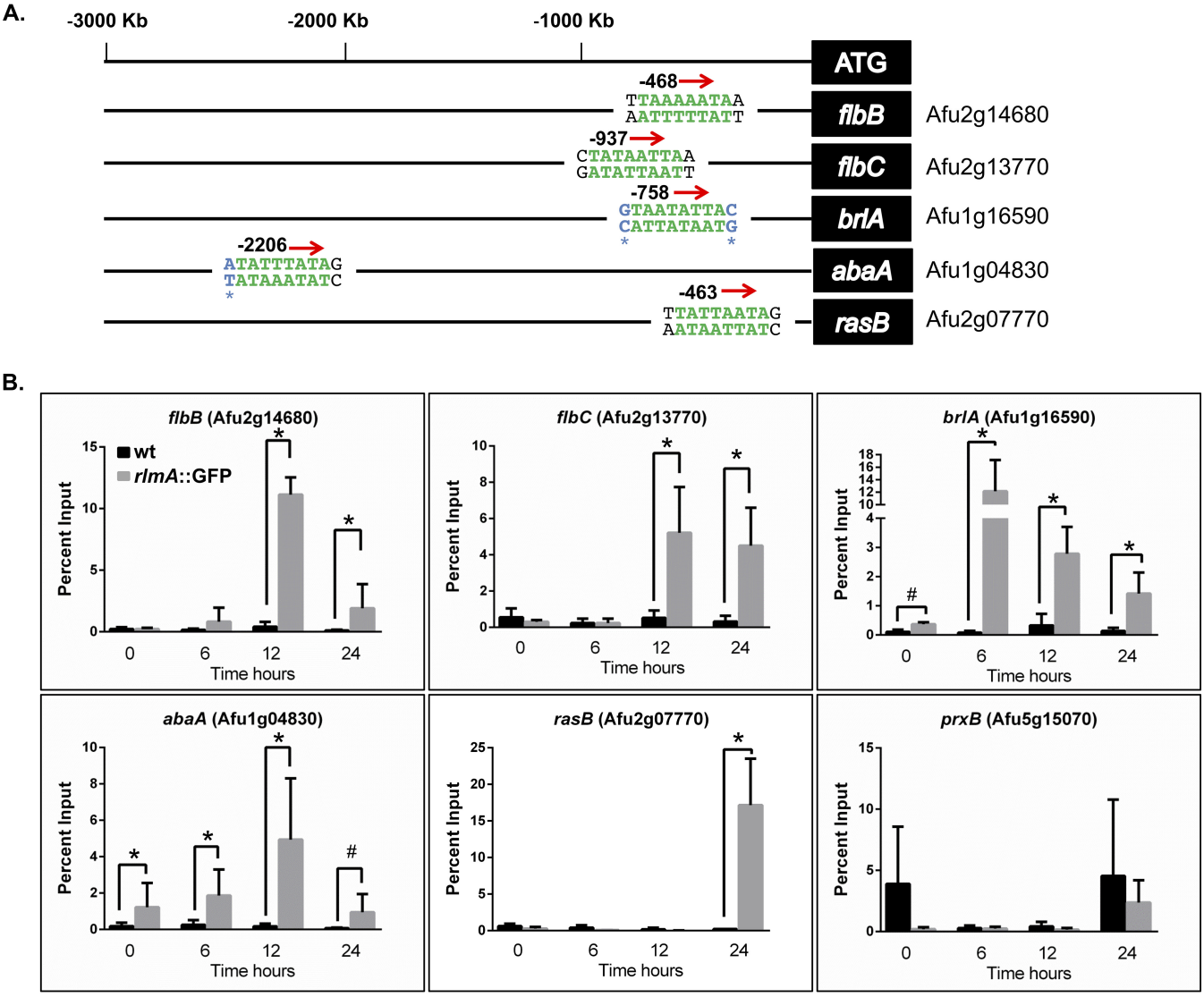

FIG 4 RlmA binds to the promoter region of central regulators of conidiation. (A) Location of RlmA binding motifs at the promoter region of the tested genes. Green letters indicate the DNA core sequence 5′-TAWWWWTA-3′ (W = A or T), while black letters indicate the described variations "Y" and "R" at the 5′ and 3′ (1st and 10th base) regions of the motif (Y = C or T; R = A or G). Blue letters indicate a single base variation observed in the binding motif at the promoter region of the *brlA* and *abaA* genes. (B) ChIP-qPCR assays of the wild-type and *rlmA*::GFP strains subjected to synchronized asexual differentiation. Graphs show the average ± the SD from three independent biological experiments (with two technical repetitions each). The percent input is the ratio of the signals obtained from the immunoprecipitated sample and the starting DNA material (input sample) used for the ChIP reaction. Statistical analysis was performed using a one-tailed, paired *t* test compared to the wild-type control condition (*, $P \leq 0.0001$; #, $P \leq 0.005$). As a negative binding control, an oligonucleotide located at an exonic region of the *prxB* gene was used (47).

binding motif, RlmA is dispensable for *rasB* expression since the mRNA abundance of *rasB* at 37°C is dramatically increased after 24 h of asexual differentiation in all three mutants, remarkably in the Δ*mpkA* and Δ*rlmA* mutants (Fig. 5B). Altogether, we interpret these findings as evidence that RlmA is essential to coordinate asexual development.

The MAPK MpkA associates with regulators of asexual development in *A. fumigatus*. To investigate further the mechanisms of CWIP and asexual development regulation, we evaluated whether MpkA contributes to the activation of the UDAs FlbB-C, the central regulator BrlA, and the late regulator RasB. To test this hypothesis, we looked for a physical interaction between these proteins and MpkA by using coimmunoprecipitation (Co-IP) experiments. Therefore, we generated several strains in which the *flbB*, *flbC*, *brlA*, and *rasB* genes were individually replaced by an allele

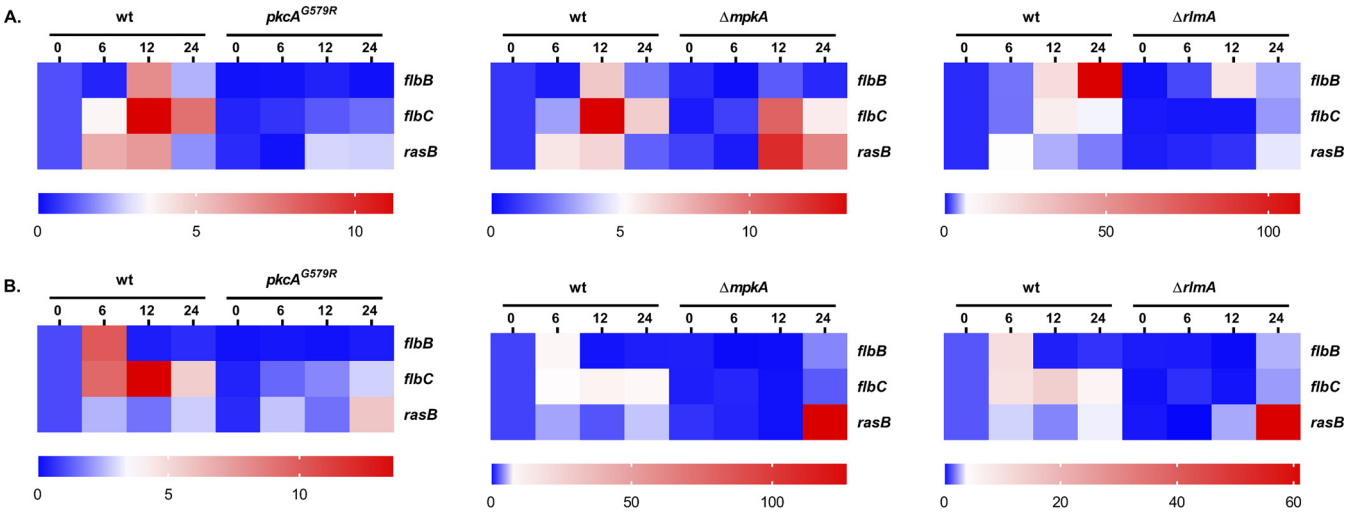

FIG 5 CWIP genes are required for the expression of *flbB* and *flbC*. The expression of *flbB*, *flbC*, and *rasB* was investigated by RT-qPCR in the strains subjected to synchronized asexual differentiation during the indicated time points (hours) at 30°C (A) and 37°C (B). Values represent the averages of results from three independent experiments with two technical repetitions each (see Fig. S7; *, $P \leq 0.01$ one-way ANOVA) and are presented as the relative expression of the mutant strain compared to the same time point of the wild-type strain.

encoding a green fluorescent protein (GFP) tag and used them to transform the cassette *mpkA*::3×HA to obtain double-tagged strains. The results of the immunoblotting analyses indicated that MpkA was recovered by coimmunoprecipitated samples from only the GFP-tagged FlbB, FlbC, BrlA, and RasB strains (Fig. 6A and B). Identical results were obtained in the reciprocal experiment where MpkA::3×HA was pulled down (Fig. 6C and D). It is worth noting that under the control condition (hyphal state), no interaction between MpkA and RasB was recorded.

RlmA controls mRNA abundance of cell wall-degrading enzymes during conidiation. To gain more insight into how CWIP and RlmA coordinate the expression of genes involved in cell wall remodeling during conidiation, we reanalyzed a data set of genes previously described as transcriptionally upregulated in a wild-type strain 24 h postinduction of asexual development (33). We focused on the 2,752 transcripts that were induced at least 2-fold and used the FungiFun tool to identify overrepresented GO terms in this data set (Data Set S3). The analysis returned 23 enriched categories, and we focused on the 63 genes belonging to the category "carbohydrate metabolic process" to identify genes annotated as chitinases, glucanases, or glycosyl hydrolases. Subsequently, we examined the presence of the RlmA binding motif in the promoter regions of the chosen genes. Table 1 summarizes the results for the selected genes that fulfill this criterion. Genes displaying very high expression levels that presented a predicted RlmA binding sequence were selected to be assayed by ChIP-qPCR. Curiously, for the genes Afu3g07160, Afu3g11280, and Afu3g07110, we observed a variation within the core DNA sequence of the motif (5′-TAWWWWTA-3′) in which the TA after the A/T stretches was replaced by a TT or TC (Fig. 7A). Considering the location of these putative binding sequences in the promoter regions, we included them in the ChIP-qPCR analyses.

We observed that the promoter regions for 9 out of 10 genes tested were significantly enriched (Fig. 7B). The only exception was the glycosyl hydrolase Afu6g08080, which presented two overlapping and fully conserved RlmA binding motifs. Consistently, the transcription of Afu6g08080 was not completely abrogated in the Δ*rlmA* background (Fig. S8). All other genes, especially *chi4*, *chi5*, *chiB1*, *nagA*, and Afu3g11280, were strongly upregulated during conidiation and fully required *rlmA* for expression (Fig. S8). Remarkably, the promoter regions of all the chitinases that possessed a predicted RlmA binding motif were bound by RlmA (Fig. 7B). Collectively, our results suggest that RlmA directly controls the transcription of chitinases and glucanases

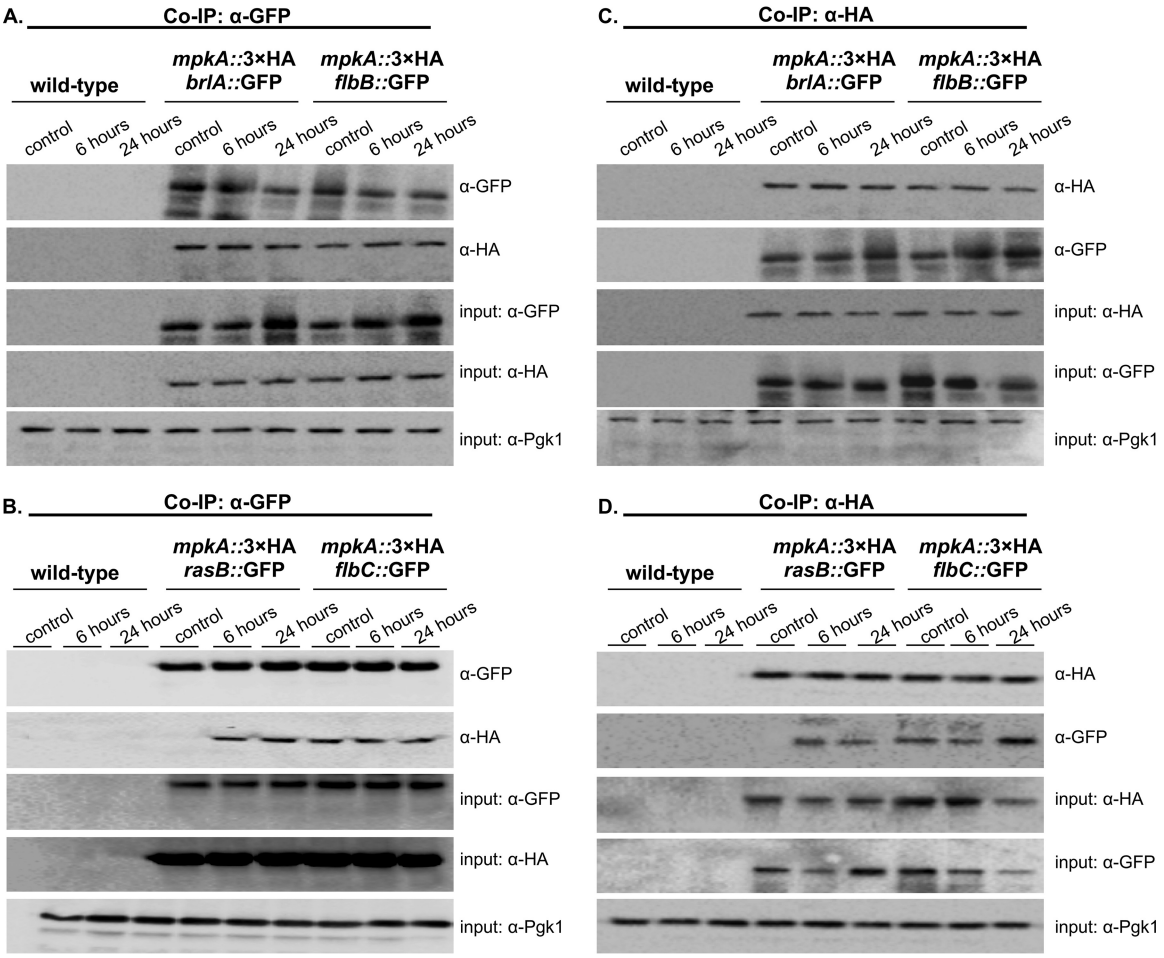

FIG 6 MpkA interacts with FlbB, FlbC, BrlA, and RasB during the early stages of conidiation. Co-IP was performed with total protein extracts from the wild-type and the respective strains expressing both GFP and the 3×HA C-terminal tag subjected to synchronized asexual differentiation at 37°C. (A and B) Co-IP experiments performed with an α-GFP antibody that specifically isolates the MpkA 3×HA protein only in the presence of the GFP-tagged proteins. (C and D) Reciprocal Co-IP experiments using an α-HA antibody to isolate the corresponding GFP-tagged proteins. α-Pgk1 was used as an input control. Predicted fusion protein sizes on the blot: FlbB::GFP, 72 kDa; FlbC::GFP, 63.2 kDa; BrlA::GFP, 74.9 kDa; RasB::GFP, 51.5 kDa; and MpkA::3×HA, 51 kDa.

during conidiation, suggesting that massive cell wall remodeling occurs during this process. This emphasizes the importance of RlmA function for both the synthesis and the degradation of the fungal cell wall in *A. fumigatus*.

DISCUSSION

Over the last decade, several studies have shed light on how CWIP impacts the regulation of diverse cellular processes, such as cell wall maintenance, secondary metabolite production, drug tolerance, and ultimately virulence in *A. fumigatus* (29, 34–37). Here, we report that the defective function of genes critical for the CWIP impairs the timing of conidiation in *A. fumigatus*. Despite the vegetative growth defect described for the Δ*mpkA* strain (12, 15), the most severe conidiation defect was observed for the Δ*rlmA* mutant, suggesting that the MpkA-dependent RlmA activity is essential for the initial stages of the asexual development. Consistently, we show that MpkA phosphorylation increases in the wild-type strain during asexual differentiation in a time-dependent manner, while MpkA phosphorylation is either lower in the *pkcA*^{G579R} mutant or almost absent in the Δ*rlmA* strain (Fig. 2). We have shown that phosphorylation of MpkA is reduced in the Δ*rlmA* mutant in response to cell wall stress (16). We initially interpreted this result as a potential positive regulatory role for *rlmA* during cell wall stress, which could intensify the activity of the CWIP. Here, our results confirm this

TABLE 1 Selected cell wall remodeling genes involved in glucan and chitin metabolism upregulated by 24 h postinduction of asexual development

Gene	Gene name	FI[a]	Putative RlmA motif (5′–3′)	Position	Description
Afu1g02800	Afu1g02800	3.6			Putative family 18 chitinase
Afu1g04260	*engl1*	19.9			β-1,3-Endoglucanase, associated with cell wall
Afu1g05290	*eng3*	5.6	TTAAAATTAC	−593	GH16 endo-1,3(4)-β-glucanase, putative
Afu1g17410	*exg15*	2.2			Putative β-glucosidase
Afu3g07110	*chi5*	9.4	TTATTTTTCC	−1391	Class III chitinase, putative
Afu3g07160	Afu3g07160	46.6	TTAWWWWT	−180	Class V chitinase, putative
Afu3g11280	Afu3g11280	7.7	TTATTAATTT/CTATTATTTA	−300/−328	Class V chitinase, putative
Afu4g13360	*eng5*	7.4			Predicted hydrolase activity, hydrolyzing O-glycosyl compounds; activity and role in carbohydrate metabolic process
Afu5g02280	*eng4*	9.4	CTATTTTTAG	−444	GH16 endo-1,3(4)-β-glucanase, putative
Afu5g03530	*chi4*	16.1	CCTAAATTTG	−2007	Class III chitinase, putative
Afu5g06840	Afu5g06840	2.9			Class V chitinase, putative
Afu5g07190	*exg18*	7.7			β-Glucosidase
Afu6g08080	Afu6g08080	23.8	TTATTAATAA/TTAATAATAA	−929/−932	Glycosyl hydrolase, putative
Afu6g08700	*exg20*	29.6			β-Glucosidase, putative
Afu6g12010	Afu6g12010	6.6			Putative β-glucosidase with a predicted role in degradation of glucans
Afu6g12380	*scw4*	78.1			Cell wall glucanase (Scw4), putative
Afu6g13720	Afu6g13720	7.5			Class V chitinase, putative
Afu7g05610	*exg3*	3.4			Glucanase, putative
Afu7g06140	*exg13*	307.2			Putative secreted 1,4-β-D-glucan glucan hydrolase
Afu8g01410	*chiB1*	498.7	TTAATATTAT	−202	Class V chitinase ChiB1
Afu8g02100	*exg16*	3.6			β-Glucosidase, putative
Afu8g02510	Afu8g02510	66.9	TTAATTATAG	−555	Predicted hydrolase activity, hydrolyzing O-glycosyl compounds; activity and role in carbohydrate metabolic process
Afu8g05020	*nagA*	79.5	GTATAATTAT	−1348	β-*N*-Acetylhexosaminidase NagA, putative

[a]FI, fold increase after 24 h of synchronized asexual differentiation assessed by RNA-seq analysis (33).

interpretation and suggest that lower MpkA phosphorylation may occur under any growth condition when RlmA function is absent. Our data also suggest that transcription levels of the *pkcA* gene are reduced in the Δ*rlmA* mutant (Fig. S4), which might cause lower levels of the PkcA protein and reduced activation of CWIP signaling. However, the underlying mechanisms that explain this effect remain undescribed. In addition, RlmA phosphorylation highly increases throughout conidiation, suggesting that the transcriptional activation elicited by RlmA is required at the start of the conidiation and is likely to become more prominent at later times of the process. Supporting this idea, we find that UDAs, CRPs, and Ras components are direct RlmA transcriptional targets.

The data presented in this study point to a particular role of MpkA and RlmA during the initial phases of conidiophore development that culminates with the observed phenotype of delayed conidiation. This outcome is consistent with the observed defects in the expression of *abaA* and *wetA* in these deletion mutants (Fig. 3). However, we found the conserved TAWWWWTA motif in *brlA* and *abaA*, but not in *wetA*, suggesting that the lack of *wetA* expression could be due to a downstream consequence of the lack of *abaA* expression and not by the absence of RlmA binding to the *wetA* promoter. RlmA binds to the promoters of *brlA* and *abaA* with maximum binding levels between 6 and 12 h after induction of conidiation, which coincides with the onset of the expression of these genes. The conserved RlmA motif was also found in the promoters of *flbB* and *flbC* but not in the promoters of other fluffy genes. Although the fluffy genes are expressed during vegetative growth (17, 18, 38), RlmA only binds to the promoters of *flbB* and *flbC* 12 to 24 h postinduction. These are the only fluffy genes present in vesicles, the metula, and phialides but not in conidia (39, 40). Therefore, MpkA and RlmA seem to be involved in the regulation of genes that participate in the formation of such structures but not necessarily in the formation of conidia. Importantly, the lack of *rlmA* results in massive reductions in *flbB* and *flbC* mRNA levels. FlbB and FlbC participate in vesicle swelling and metula development together with BrlA (38), but the roles of these genes during these conidiation phases

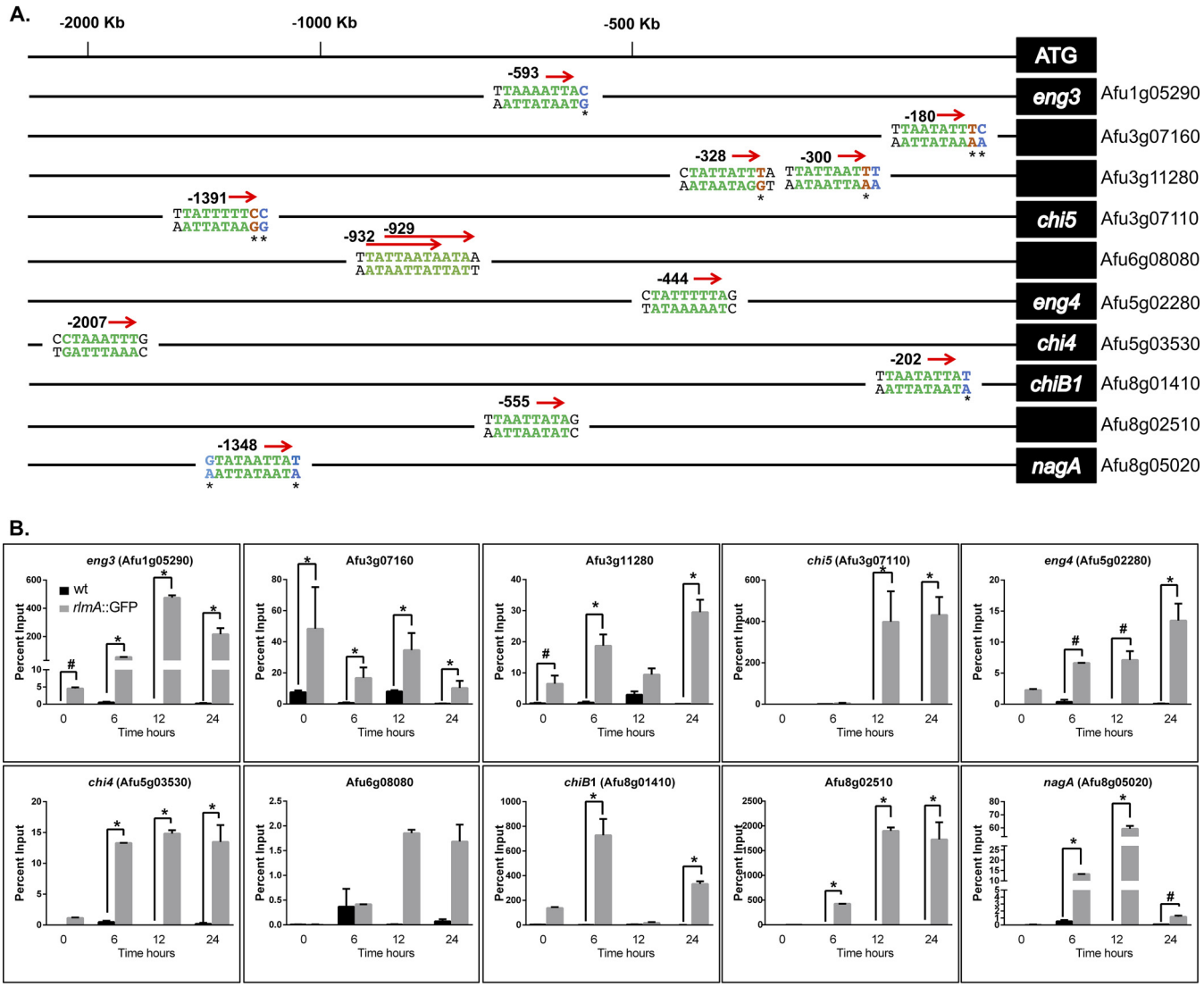

FIG 7 RlmA binds to the promoter region of chitinase and glucanase genes during conidiation. (A) Location of predicted RlmA binding motifs in the promoter region of the tested genes. Green letters indicate the DNA core sequence 5′-TAWWWWTA-3′ (W = A or T), and red letters indicate a variation within this core sequence. Black letters indicate the described variation at Y and R position (1st and 10th base) regions of the motif (Y = C or T; R = A or G). Blue letters indicate a variation observed at the Y or R position. (B) ChIP-qPCR assays of the wild-type and *rlmA*::GFP strains subjected to synchronized asexual differentiation. Graphs show the averages ± the SD from three independent biological experiments (with two technical repetitions each). Statistical analysis was performed using a one-tailed, paired *t* test compared to the control condition (*, $P \leq 0.0001$; #, $P \leq 0.005$).

are still unknown. These events require cell wall remodeling, but since the conidiophore morphology is normal (Fig. S3), it is possible that the lack of transcriptional activation promoted by RlmA or the lack of MpkA-mediated phosphorylation on the target genes identified here is not sufficient to produce detectable abnormalities in the conidiophore stalks but is sufficient to impair the timely emergence of conidia. One explanation is that this may be a function of delayed onset rather than the rate of asexual development or conidial production. The slopes of all the curves shown in Fig. 1 are reasonably similar, so the kinetics of conidiation are comparable, although the effect is lower conidia number. Future experiments in strains carrying mutations in the identified binding sites will provide information about the individual contribution of RlmA in the activation of FlbB-C, BrlA, and AbaA in conidiation.

The function of the CWIP during conidiation suggests that the typical structural organization of carbohydrate in the *A. fumigatus* conidia can be highly dependent on this cascade. RlmA regulates the expression of genes related to cell wall biosynthesis,

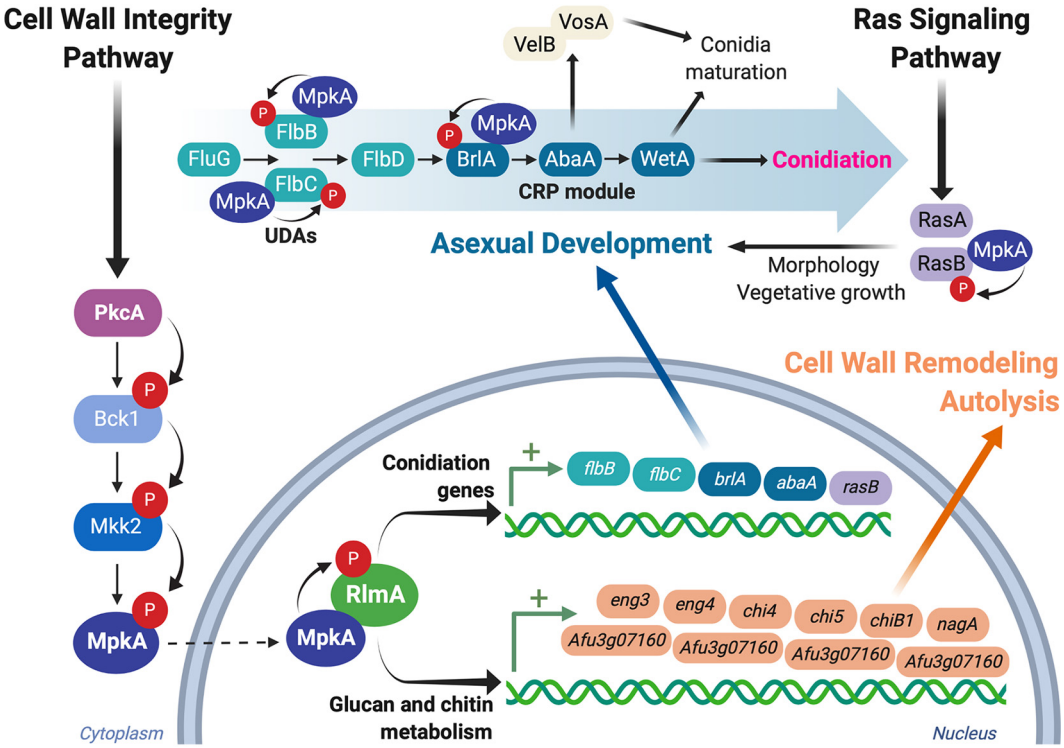

FIG 8 The CWI pathway contributes to the regulation of the conidiation onset and cell wall remodeling during asexual differentiation. The CWI pathway is activated during the initial stages of asexual competence and culminates with the phosphorylation and activation of the MAP kinase MpkA (red circles). MpkA migrates to the nucleus and phosphorylates RlmA (the details on the interaction between MpkA and RlmA will be published elsewhere). Active RlmA participates in the control of the metabolic changes that take place during the asexual differentiation via the activation of two distinct sets of genes. (i) RlmA binds to the promoter regions of genes involved in conidiation, including the UDAs *flbB* and *flbC* and the CRP genes *brlA* and *abaA*, allowing timely transcription of such regulators. In addition, the Ras signaling pathway is activated late in the cascade. (ii) RlmA binds to the promoter regions of several genes involved in glucan and chitin metabolism. These enzymes can act on the cell wall (not shown) to cause cell wall remodeling aiming to adapt cells to the formation of aerial structures and conidiation or to induce autolysis, thus contributing to the supply of nutrients required for conidiation. In an additional regulatory event, the active MpkA in the cytosol physically associates with proteins involved in the conidiation pathway. Collectively, the combined actions of activated MpkA and RlmA coordinate alterations in the cell wall composition and timely expression of UDAs and CRP, contributing to the formation of conidia and vegetative growth. The organization of the conidiation pathway was based on references (20, 27, 41). This image was created using BioRender.

and we found an increase in the chitin content in aerial hyphae of the Δ*rlmA* strain (16). All these processes that occur during conidiophore development required the reorganization of the cell wall, i.e., erection of the stalk, the swelling of the vesicle, and budding of the metula and phialides. We hypothesize that *rlmA* and *mpkA* cooperate at the cross talk between cell wall formation and the regulation of conidiophore development by coregulating the expression of the conidiation regulators and glucan and chitin metabolic genes, participating until the formation of the phialides. The formation of the conidial cell wall is, however, a downstream process during the life cycle of the fungus; it requires *wetA*, which is not a RlmA direct target but is also controlled by a completely different set of regulators, such as *vosA* and *velB*, (25, 41) that are not investigated here (Fig. 8).

It has been demonstrated in *A. nidulans* that RlmA regulates the expression of glucanases and chitinases, which are thought to promote autolysis in submerged cultures (42). Our results also demonstrate that RlmA regulates the expression of genes involved in cell wall remodeling and autolysis during asexual differentiation. The production of extracellular autolytic enzymes such as chitinase and glucanase is induced by carbon starvation in *A. nidulans* (43). Intriguingly, the strain defective in both *chiB* and *engA* produced fewer conidia on medium containing low concentrations of glucose (44). This observation indicates that autolysis contributes to the supply of

TABLE 2 *A. fumigatus* strains used in this study

Strain	Relevant genotype[a]	Source or reference
ΔKU80 pyrG1	Δ*akuB*; *pyrG*-MAT1-1	60
Δ*rlmA*	Δ*rlmA*::*pyrG*; Δ*akuB*	16
Δ*rlmA*::*rlmA*$^+$	Δ*rlmA*::*rlmA*$^+$; Δ*akuB*	16
rlmA::3×FLAG	*rlmA*::3×FLAG::*pyrG*; Δ*akuB*	This study
rlmA::GFP	*rlmA*::GFP::*pyrG*; Δ*akuB*	16
pkcA^{G579R}	*pkcA*^{G579R}::*pyrG*; Δ*akuB*	11
pkcA^{G579R}::*pkcA*$^+$	*pkcA*^{G579R}::*pkcA*$^+$; Δ*akuB*	11
Δ*mpkA*	Δ*mpkA*::*prtA*; Δ*akuB*, PtrA$^+$	12
Δ*mpkA*::*mpkA*$^+$	Δ*mpkA*::*mpkA*$^+$; Δ*akuB*	12
flbB::GFP *mpkA*::3×HA	*flbB*::GFP::*pyrG*; *mpkA*::3×HA::*ptrA*; Δ*akuB*; Pt^r	This study
flbC::GFP *mpkA*::3×HA	*flbC*::*GFP*::*pyrG*; *mpkA*::3×HA::*ptrA*; Δ*akuB*; Pt^r	This study
brlA::GFP *mpkA*::3×HA	*brlA*::GFP::*pyrG*; *mpkA*::3×HA::*ptrA*; Δ*akuB*; Pt^r	This study
rasB::GFP *mpkA*::3×HA	*rasB*::GFP::*pyrG*; *mpkA*::3×HA::*ptrA*; Δ*akuB*; Pt^r	This study

[a]Pt^r, pyrithiamine resistant.

nutrients required for conidiation. The corresponding genes, *chiB1* and *engl1*, were highly induced during conidiation in wild-type *A. fumigatus*, although only *chiB1* is a RlmA target (Table 1 and Fig. 7). From these results, we suggest that cell wall remodeling is a crucial process that takes place during conidiation. It is tempting to assume that RlmA coordinately regulates the induction of autolytic enzymes to provoke autolysis and conidiation, although further clarification is required.

In summary, this study demonstrates the participation of CWIP in the progression of conidiogenesis in *Aspergillus*. This highlights the complexity underlying cell wall remodeling during asexual differentiation in filamentous fungi coupled with the multitude of signaling pathways involved in the regulation of such processes. We argue that the ability of RlmA to bind to the promoters of conidiation genes as well as glucanases and chitinases and the physical interaction between MpkA and FlbB, FlbC, BrlA, and RasB are key events required for conidiation timing. Especially in the case of MpkA-mediated phosphorylation of the developmental regulators highlighted here, the specific residues that undergo phosphorylation and the impact of these events on the conidiation remain to be determined.

MATERIALS AND METHODS

Strains and culture conditions. The *A. fumigatus* strains used in this study are described in Table 2. All the strains were maintained in complete medium or minimal medium as described previously (45). To grow the Δ*akuB pyrG1* strain, the medium was supplemented with 1.2 g/liter uridine and uracil. Synchronized asexual differentiation was conducted as described previously (46). Briefly, 1×10^8 conidia of the wild-type, *pkcA*^{G579R}, or Δ*rlmA* strains were inoculated in 100 ml of liquid minimal medium supplemented with 0.1% yeast extract and incubated at 37°C (200 rpm) for 18 h (Fig. S2). For the Δ*mpkA* mutant, the amount of conidia used was four times that of the wild-type strain to achieve equal glucose consumption (35). Mycelia from the submerged cultures (5 g [wet weight]) were then harvested by filtration and flash frozen in liquid nitrogen or transferred to solid complete medium and further incubated at 30°C (for 12, 24, and 36 h) or at 37°C (for 6, 12, and 24 h). Mycelia obtained from the submerged cultures (hyphal state) were considered the control condition for the experiments. Samples were collected at each time point and stored at −80°C until they were used for either RNA or protein extractions. To visualize the conidiophores of the CWIP mutants, we used a slide culture as previously described (11).

Construction of GFP-, 3×FLAG-, and 3×HA-tagged strains. All gene replacement cassettes were constructed by *in vivo* recombination in *S. cerevisiae*, as reported previously (45). The *flbB*::GFP, *flbC*::GFP, *brlA*::GFP, and *rasB*::GFP cassettes were generated using the primers and strategies described in Table S1 and Fig. S9, respectively, in the supplemental material. The GFP::*pyrG* cassette employed in these constructs was amplified from plasmids described earlier (47). The *mpkA*::3×HA::*ptrA* cassette was amplified from the plasmid pUC19-mpkA::3×HA (48) and transformed into *flbB*::GFP, *flbC*::GFP, *brlA*::GFP, and *rasB*::GFP strains to obtain double-tagged alleles. To construct the *rlmA*::3×FLAG strain, a substitution cassette was obtained in which the *rlmA* genomic sequence without stop codon was cloned in-frame with the 3×FLAG in a C-terminal fusion separated by a $(GA)_5$ linker fused with the *pyrG* gene a selection marker. All gene replacements were confirmed by PCR with the primers described in Fig. S9. We observed no changes in the phenotypes of the tagged strains compared to wild-type (Fig. S10).

Quantification of conidia during asexual development. Conidial counts for each strain subjected to synchronized asexual differentiation at 30 or 37°C were performed by sampling 0.5 g of mycelium at 2-h intervals for up to 48 h. The conidia were collected in 0.01% Tween 20 solution and counted in a Neubauer chamber. Experiments were repeated three times.

Analysis of hydrophobic properties of conidia and rodlet layer extraction. The distribution of the conidia on a water-oil interface was performed by the addition of 1×10^8 conidia of each strain in a solution containing water and tributyrin (1:1 [vol/vol]) as described previously (49). The hydrophobins were extracted from the dormant conidia surface by incubating freshly harvested conidia with 48% hydrofluoric acid for 72 h at 4°C according to the previous description (11, 50).

Chitin content determination during asexual development. Continuous photometric reading and parallel quantification of hyphal growth and fluorophore detection directly on solid medium was used as described previously (30). Briefly, conidia from each strain were inoculated on solid media in a 96-well plate, followed by incubation at 37°C for different periods to cover an ample spectrum of growth. Then, 150 μl of CFW stock solution (10 μg/ml 10 mM Tris HCl [pH 8], 0.1% Tween 80) was added to each well. The fluorescence (excitation, 360 nm; emission, 460 nm) and the absorbance at 600 nm were measured in a BioTek HTX multimode plate reader. Fluorescence was plotted against the absorbance for each strain, and the slope was calculated. The experiment was repeated four times with technical duplicates.

RNA extraction and RT-qPCR analysis. Samples from the synchronized asexual differentiation obtained at 30 and 37°C were disrupted, and the total RNA obtained was extracted and processed for cDNA synthesis as previously described (11, 51). The primers for the individual genes are listed in Table S2. At least three independent biological replicates were used for each condition and the relative fold change for each gene was calculated using comparative cycle threshold (C_T), i.e., $\Delta\Delta C_T$, analysis (52). All values were normalized to the expression of the *A. fumigatus tubA* gene. Statistical analysis was performed by using one-way analysis of variance (ANOVA) with a Tukey's post *hoc test* to assess differences in the mutant strains compared to the same developmental time point in the wild-type strain ($P \leq 0.05$).

Global MADS box motif identification. The analysis of promoter regions was performed based on previous reports describing the predicted conserved poly A/T stretches (5′-TAWWWWTA-3′; W = A or T), which are recognized by the MADS-box RlmA transcription factors of *A. niger*, *A. nidulans*, and *A. fumigatus* (29, 42, 53) and conserved with *S. cerevisiae* Rlm1 (32). We also took into account the vicinity of the motif core, which included the 5′-YTAWWWWTAR-3′ (Y = C or T; R = A or G) or 5′-YTAWWWWT AN-3′ sequences, as previously reported (29, 32, 54). Motifs were identified using the *ad hoc* scripts written in *Perl*. For this, a fasta file with 9,841 promoter sequences was screened for the putative MADS-box motif using regular expressions. Putative binding sites localized between positions −1000 to −1 were initially identified. Manual inspection of the putative binding sites located between −3000 and −1 was also conducted for *brlA*, *abaA*, and *wetA* and the chitin-metabolizing genes *chi5*, *chiB1*, and *nagA*, which were previously found to be putative RlmA transcriptional targets in *A. nidulans* (42).

Chromatin immunoprecipitation coupled to qPCR. The wild-type and *rlmA*::GFP strains were subjected to the synchronized asexual differentiation protocol (37°C). Cross-linking and sonication of the samples were carried out as described previously (55) with slight modifications in the sample volumes. Samples were processed as described previously (34, 55). Samples (2 ml) were sonicated for 15 cycles of 30 s, each using an Ultrasonic processor VCX-500 (Sonics & Materials), centrifuged for 5 min at 4°C, and stored at −80°C. Sonication was evaluated by using 60 μl of reverse cross-linked material for each sample, which was analyzed in agarose gel to detect bands in the range of 200 to 600 bp. Immunoprecipitation was then carried out with 900 μl of the sonicated sample and 20 μl of GFP-Trap (ChromoTek). The resin was equilibrated three times and incubated with the samples for 4 h (4°C). Sample washes and reverse cross-linking were performed as described previously (34). Relative signal abundance in regions of interest in sample DNA was measured by qPCR using Power SYBR (Thermo Fisher). The qPCRs were carried out using 0.5 μl of sonicated and purified DNA per reaction (34). Primers flanking the predicted RlmA binding motif were designed to amplify the promoter regions of the target genes (Table S3). Cross-linked and sonicated samples (nonimmunoprecipitated) were used as positive controls (input). The relative signal enrichment was calculated and normalized according to the percent input method (34).

Protein extraction and immunoblot analyses. For protein extraction, 0.5 ml of lysis buffer, as described previously (12), and 1× Complete-Mini protease inhibitor (Roche) were added to the ground mycelium. Extracts were centrifuged at 20,000 × *g* for 40 min at 4°C. The supernatants were collected, and the protein concentrations were determined using Lowry's modified method (56). Fifty micrograms of protein from each sample was resolved in a 12% (wt/vol) SDS-PAGE and transferred to polyvinylidene difluoride membranes (Bio-Rad). To assess MpkA phosphorylation, protein extracts were subjected to immunoblotting procedures described previously using α-phospho p44/42 and α-p44/42 MAPK antibodies (11, 51). Western blot signals were quantitated using ImageJ (National Institutes of Health) and normalized to total MpkA protein levels. To assess the presence of phosphorylated RlmA during asexual development, samples were separated on Phos-tag acrylamide gels. Proteins were extracted according to the manufacturer's recommendations and as described earlier (57). Phos-tag acrylamide gels consisted of 8% SDS-PAGE gels containing 100 μM Phos-tag acrylamide AAL-107 (Wako Chemicals) and 100 μM $MnCl_2$. To verify phosphate-specific signals, samples were treated with 100 U of calf intestinal alkaline phosphatase (New England Biolabs, M0290) for 40 min (37°C), followed by boiling in 1× Laemmli sample buffer. Protein samples were loaded and separated on either Phos-tag or regular 8% SDS-PAGE gels and electroblotted onto a polyvinylidene difluoride membrane.

Detection of RlmA::3×FLAG and MpkA::3×HA was achieved by using mouse α-FLAG (Sigma, F1804) or α-HA (Sigma, H3663), respectively, in Tris-buffered saline/Tween (TBST) with 3% skimmed milk at a 1:1,000 dilution with overnight incubation (4°C). GFP was detected using a mouse monoclonal α-GFP primary antibody (Santa Cruz Biotechnology, sc-9996) at a 1:1,000 dilution in TBST with 3% skimmed milk (4°C overnight). Secondary α-mouse IgG-HRP antibody (Sigma, A4416) in TBST (1:3,000 dilution) was used for a 2-h incubation period at room temperature. Goat α-γ-tubulin (Santa Cruz Biotechnology, γN-20)

was used as loading control under conditions previously indicated (47). Chemiluminescent detection for each antibody was achieved by using an ECL Prime western blot detection kit (GE HealthCare). Images were generated by exposing the membranes to the ChemiDoc XRS gel imaging system (Bio-Rad).

Coimmunoprecipitation assays. The double-tagged strains containing both in-frame GFP fusions with either *rasB*, *flbB*, *flbC*, or *brlA* and 3×HA with *mpkA* were used. For GFP-Trap Co-IP, experiments were performed by using 20 μl of GFP-trap and 5 mg of protein, which were extracted and processed for IP as described elsewhere (34). For reciprocal Co-IP using α-HA affinity gel (EzView; Sigma, E6779), samples were extracted using B250 buffer (58) and processed for immunoprecipitation as described previously (59), using 30 μl of resin and 5 mg of protein. Hemagglutinin (HA) resin was centrifuged for 30 s (13,000 × *g*) for recovery and washed with B250 buffer. For both procedures, proteins were released from resin by boiling in 30 μl of 2× Laemmli buffer. Portions (20 μl) of each sample were run on a 10% SDS-PAGE gel. The proteins were electroblotted and detected as described above.

SUPPLEMENTAL MATERIAL

Supplemental material is available online only.

SUPPLEMENTAL FILE 1, PDF file, 13.4 MB.

SUPPLEMENTAL FILE 2, XLSX file, 0.04 MB.

SUPPLEMENTAL FILE 3, XLSX file, 0.1 MB.

SUPPLEMENTAL FILE 4, XLSX file, 0.7 MB.

ACKNOWLEDGMENTS

We thank Robert A. Cramer for critical reading of the manuscript and the three anonymous reviewers and the editor for their comments and suggestions. We are also indebted to Vito Valiante for providing the Δ*mpkA* strain and Maria J. P. Bezerra for technical support (FAPESP 2018/01442-0).

We thank FAPESP (Fundação de Amparo à Pesquisa do Estado de São Paulo [2015/17541-0, 2016/07870-9, and 2017/19694-3]) and CNPq (Conselho Nacional de Desenvolvimento Científico e Tecnológico [462383/2014-8]) for funding. The funders had no role in study design, data collection and interpretation, or the decision to submit the work for publication.

REFERENCES

1. Tekaia F, Latge JP. 2005. *Aspergillus fumigatus*: saprophyte or pathogen? Curr Opin Microbiol 8:385–392. https://doi.org/10.1016/j.mib.2005.06.017.
2. Brown GD, Denning DW, Gow NA, Levitz SM, Netea MG, White TC. 2012. Hidden killers: human fungal infections. Sci Transl Med 4:165rv13. https://doi.org/10.1126/scitranslmed.3004404.
3. Kwon-Chung KJ, Sugui JA. 2013. *Aspergillus fumigatus*: what makes the species a ubiquitous human fungal pathogen? PLoS Pathog 9:e1003743. https://doi.org/10.1371/journal.ppat.1003743.
4. Latge JP. 1999. *Aspergillus fumigatus* and aspergillosis. Clin Microbiol Rev 12:310–350. https://doi.org/10.1128/CMR.12.2.310.
5. Taha MP, Pollard SJ, Sarkar U, Longhurst P. 2005. Estimating fugitive bioaerosol releases from static compost windrows: feasibility of a portable wind tunnel approach. Waste Manag 25:445–450. https://doi.org/10.1016/j.wasman.2005.02.013.
6. Sugui JA, Kwon-Chung KJ, Juvvadi PR, Latgé J-P, Steinbach WJ. 2014. *Aspergillus fumigatus* and related species. Cold Spring Harb Perspect Med 5:a019786. https://doi.org/10.1101/cshperspect.a019786.
7. Abad A, Fernandez-Molina JV, Bikandi J, Ramirez A, Margareto J, Sendino J, Hernando FL, Ponton J, Garaizar J, Rementeria A. 2010. What makes *Aspergillus fumigatus* a successful pathogen? Genes and molecules involved in invasive aspergillosis. Rev Iberoam Micol 27:155–182. https://doi.org/10.1016/j.riam.2010.10.003.
8. van de Veerdonk FL, Gresnigt MS, Romani L, Netea MG, Latgé J-P. 2017. *Aspergillus fumigatus* morphology and dynamic host interactions. Nat Rev Microbiol 15:661–674. https://doi.org/10.1038/nrmicro.2017.90.
9. Latge JP, Beauvais A, Chamilos G. 2017. The cell wall of the human fungal pathogen *Aspergillus fumigatus*: biosynthesis, organization, immune response, and virulence. Annu Rev Microbiol 71:99–116. https://doi.org/10.1146/annurev-micro-030117-020406.
10. Levin DE. 2011. Regulation of cell wall biogenesis in *Saccharomyces cerevisiae*: the cell wall integrity signaling pathway. Genetics 189:1145–1175. https://doi.org/10.1534/genetics.111.128264.
11. Rocha MC, Godoy KF, de Castro PA, Hori JI, Bom VL, Brown NA, Cunha AF, Goldman GH, Malavazi I. 2015. The *Aspergillus fumigatus pkcA* G579R mutant is defective in the activation of the cell wall integrity pathway but is dispensable for virulence in a neutropenic mouse infection model. PLoS One 10:e0135195. https://doi.org/10.1371/journal.pone.0135195.
12. Valiante V, Jain R, Heinekamp T, Brakhage AA. 2009. The MpkA MAP kinase module regulates cell wall integrity signaling and pyomelanin formation in *Aspergillus fumigatus*. Fungal Genet Biol 46:909–918. https://doi.org/10.1016/j.fgb.2009.08.005.
13. Dichtl K, Helmschrott C, Dirr F, Wagener J. 2012. Deciphering cell wall integrity signaling in *Aspergillus fumigatus*: identification and functional characterization of cell wall stress sensors and relevant Rho GTPases. Mol Microbiol 83:506–519. https://doi.org/10.1111/j.1365-2958.2011.07946.x.
14. Samantaray S, Neubauer M, Helmschrott C, Wagener J. 2013. Role of the guanine nucleotide exchange factor Rom2 in cell wall integrity maintenance of *Aspergillus fumigatus*. Eukaryot Cell 12:288–298. https://doi.org/10.1128/EC.00246-12.
15. Valiante V, Heinekamp T, Jain R, Hartl A, Brakhage AA. 2008. The mitogen-activated protein kinase MpkA of *Aspergillus fumigatus* regulates cell wall signaling and oxidative stress response. Fungal Genet Biol 45:618–627. https://doi.org/10.1016/j.fgb.2007.09.006.
16. Rocha MC, Fabri JH, Godoy KF, Castro PA, Hori JI, Cunha AF, Arentshorst M, Ram AF, van den Hondel CA, Goldman GH, Malavazi I. 2016. *Aspergillus fumigatus* MADS-Box transcription factor *rlmA* is required for regulation of the cell wall integrity and virulence. G3 (Bethesda) 6:2983–3002. https://doi.org/10.1534/g3.116.031112.
17. Adams TH, Wieser JK, Yu JH. 1998. Asexual sporulation in *Aspergillus nidulans*. Microbiol Mol Biol Rev 62:35–54. https://doi.org/10.1128/MMBR.62.1.35-54.1998.
18. Yu JH. 2010. Regulation of development in *Aspergillus nidulans* and *Aspergillus fumigatus*. Mycobiology 38:229–237. https://doi.org/10.4489/MYCO.2010.38.4.229.
19. Park HS, Yu JH. 2016. Developmental regulators in *Aspergillus fumigatus*. J Microbiol 54:223–231. https://doi.org/10.1007/s12275-016-5619-5.
20. Krijgsheld P, Bleichrodt R, van Veluw GJ, Wang F, Müller WH, Dijksterhuis

J, Wösten HAB. 2013. Development in *Aspergillus*. Stud Mycol 74:1–29. https://doi.org/10.3114/sim0006.
21. Etxebeste O, Ni M, Garzia A, Kwon NJ, Fischer R, Yu JH, Espeso EA, Ugalde U. 2008. Basic-zipper-type transcription factor FlbB controls asexual development in *Aspergillus nidulans*. Eukaryot Cell 7:38–48. https://doi.org/10.1128/EC.00207-07.
22. Mah JH, Yu JH. 2006. Upstream and downstream regulation of asexual development in *Aspergillus fumigatus*. Eukaryot Cell 5:1585–1595. https://doi.org/10.1128/EC.00192-06.
23. Mirabito PM, Adams TH, Timberlake WE. 1989. Interactions of three sequentially expressed genes control temporal and spatial specificity in *Aspergillus* development. Cell 57:859–868. https://doi.org/10.1016/0092-8674(89)90800-3.
24. Ojeda-López M, Chen W, Eagle CE, Gutiérrez G, Jia WL, Swilaiman SS, Huang Z, Park H-S, Yu J-H, Cánovas D, Dyer PS. 2018. Evolution of asexual and sexual reproduction in the aspergilli. Stud Mycol 91:37–59. https://doi.org/10.1016/j.simyco.2018.10.002.
25. Tao L, Yu JH. 2011. AbaA and WetA govern distinct stages of *Aspergillus fumigatus* development. Microbiology 157:313–326. https://doi.org/10.1099/mic.0.044271-0.
26. Yu JH, Mah JH, Seo JA. 2006. Growth and developmental control in the model and pathogenic aspergilli. Eukaryot Cell 5:1577–1584. https://doi.org/10.1128/EC.00193-06.
27. Alkhayyat F, Chang Kim S, Yu JH. 2015. Genetic control of asexual development in *Aspergillus fumigatus*. Adv Appl Microbiol 90:93–107. https://doi.org/10.1016/bs.aambs.2014.09.004.
28. Wu MY, Mead ME, Lee MK, Ostrem Loss EM, Kim SC, Rokas A, Yu JH. 2018. Systematic dissection of the evolutionarily conserved WetA developmental regulator across a genus of filamentous fungi. mBio 9:e01130-18. https://doi.org/10.1128/mBio.01130-18.
29. Valiante V, Baldin C, Hortschansky P, Jain R, Thywißen A, Straßburger M, Shelest E, Heinekamp T, Brakhage AA. 2016. The *Aspergillus fumigatus* conidial melanin production is regulated by the bifunctional bHLH DevR and MADS-box RlmA transcription factors. Mol Microbiol 102:321–335. https://doi.org/10.1111/mmi.13462.
30. Canovas D, Studt L, Marcos AT, Strauss J. 2017. High-throughput format for the phenotyping of fungi on solid substrates. Sci Rep 7:4289. https://doi.org/10.1038/s41598-017-03598-9.
31. Fortwendel JR, Panepinto JC, Seitz AE, Askew DS, Rhodes JC. 2004. *Aspergillus fumigatus rasA* and *rasB* regulate the timing and morphology of asexual development. Fungal Genet Biol 41:129–139. https://doi.org/10.1016/j.fgb.2003.10.004.
32. de Boer CG, Hughes TR. 2012. YeTFaSCo: a database of evaluated yeast transcription factor sequence specificities. Nucleic Acids Res 40:D169–D179. https://doi.org/10.1093/nar/gkr993.
33. Hagiwara D, Suzuki S, Kamei K, Gonoi T, Kawamoto S. 2014. The role of AtfA and HOG MAPK pathway in stress tolerance in conidia of *Aspergillus fumigatus*. Fungal Genet Biol 73:138–149. https://doi.org/10.1016/j.fgb.2014.10.011.
34. Ries LN, Beattie SR, Espeso EA, Cramer RA, Goldman GH. 2016. Diverse regulation of the CreA carbon catabolite repressor in *Aspergillus nidulans*. Genetics 203:335–352. https://doi.org/10.1534/genetics.116.187872.
35. Jain R, Valiante V, Remme N, Docimo T, Heinekamp T, Hertweck C, Gershenzon J, Haas H, Brakhage AA. 2011. The MAP kinase MpkA controls cell wall integrity, oxidative stress response, gliotoxin production, and iron adaptation in *Aspergillus fumigatus*. Mol Microbiol 82:39–53. https://doi.org/10.1111/j.1365-2958.2011.07778.x.
36. Muller S, Baldin C, Groth M, Guthke R, Kniemeyer O, Brakhage AA, Valiante V. 2012. Comparison of transcriptome technologies in the pathogenic fungus *Aspergillus fumigatus* reveals novel insights into the genome and MpkA-dependent gene expression. BMC Genomics 13:519. https://doi.org/10.1186/1471-2164-13-519.
37. Altwasser R, Baldin C, Weber J, Guthke R, Kniemeyer O, Brakhage AA, Linde J, Valiante V. 2015. Network modeling reveals cross talk of MAP kinases during adaptation to caspofungin stress in *Aspergillus fumigatus*. PLoS One 10:e0136932. https://doi.org/10.1371/journal.pone.0136932.
38. Etxebeste O, Garzia A, Espeso EA, Ugalde U. 2010. *Aspergillus nidulans* asexual development: making the most of cellular modules. Trends Microbiol 18:569–576. https://doi.org/10.1016/j.tim.2010.09.007.
39. Etxebeste O, Herrero-García E, Araújo-Bazán L, Rodríguez-Urra AB, Garzia A, Ugalde U, Espeso EA. 2009. The bZIP-type transcription factor FlbB regulates distinct morphogenetic stages of colony formation in *Aspergillus nidulans*. Mol Microbiol 73:775–789. https://doi.org/10.1111/j.1365-2958.2009.06804.x.
40. Kwon NJ, Garzia A, Espeso EA, Ugalde U, Yu JH. 2010. FlbC is a putative nuclear C_2H_2 transcription factor regulating development in *Aspergillus nidulans*. Mol Microbiol 77:1203–1219. https://doi.org/10.1111/j.1365-2958.2010.07282.x.
41. Park HS, Bayram O, Braus GH, Kim SC, Yu JH. 2012. Characterization of the velvet regulators in *Aspergillus fumigatus*. Mol Microbiol 86:937–953. https://doi.org/10.1111/mmi.12032.
42. Kovacs Z, Szarka M, Kovacs S, Boczonadi I, Emri T, Abe K, Pocsi I, Pusztahelyi T. 2013. Effect of cell wall integrity stress and RlmA transcription factor on asexual development and autolysis in *Aspergillus nidulans*. Fungal Genet Biol 54:1–14. https://doi.org/10.1016/j.fgb.2013.02.004.
43. Emri T, Molnar Z, Szilagyi M, Pocsi I. 2008. Regulation of autolysis in *Aspergillus nidulans*. Appl Biochem Biotechnol 151:211–220. https://doi.org/10.1007/s12010-008-8174-7.
44. Emri T, Vekony V, Gila B, Nagy F, Forgacs K, Pocsi I. 2018. Autolytic hydrolases affect sexual and asexual development of *Aspergillus nidulans*. Folia Microbiol (Praha) 63:619–626. https://doi.org/10.1007/s12223-018-0601-8.
45. Malavazi I, Goldman GH. 2012. Gene disruption in *Aspergillus fumigatus* using a PCR-based strategy and *in vivo* recombination in yeast. Methods Mol Biol 845:99–118. https://doi.org/10.1007/978-1-61779-539-8_7.
46. Soriani FM, Malavazi I, da Silva Ferreira ME, Savoldi M, Von Zeska Kress MR, de Souza Goldman MH, Loss O, Bignell E, Goldman GH. 2008. Functional characterization of the *Aspergillus fumigatus* CRZ1 homologue, CrzA. Mol Microbiol 67:1274–1291. https://doi.org/10.1111/j.1365-2958.2008.06122.x.
47. Rocha MC, de Godoy KF, Bannitz-Fernandes R, Fabri J, Barbosa MMF, de Castro PA, Almeida F, Goldman GH, da Cunha AF, Netto LES, de Oliveira MA, Malavazi I. 2018. Analyses of the three 1-Cys peroxiredoxins from *Aspergillus fumigatus* reveal that cytosolic Prx1 is central to H_2O_2 metabolism and virulence. Sci Rep 8:12314. https://doi.org/10.1038/s41598-018-30108-2.
48. Manfiolli AO, Siqueira FS, dos Reis TF, Van Dijck P, Schrevens S, Hoefgen S, Föge M, Straßburger M, de Assis LJ, Heinekamp T, Rocha MC, Janevska S, Brakhage AA, Malavazi I, Goldman GH, Valiante V. 2019. Mitogen-activated protein kinase cross-talk interaction modulates the production of melanins in *Aspergillus fumigatus*. mBio 10:e00215-19. https://doi.org/10.1128/mBio.00215-19.
49. Bom VL, de Castro PA, Winkelstroter LK, Marine M, Hori JI, Ramalho LN, dos Reis TF, Goldman MH, Brown NA, Rajendran R, Ramage G, Walker LA, Munro CA, Rocha MC, Malavazi I, Hagiwara D, Goldman GH. 2015. The *Aspergillus fumigatus sitA* phosphatase homologue is important for adhesion, cell wall integrity, biofilm formation, and virulence. Eukaryot Cell 14:728–744. https://doi.org/10.1128/EC.00008-15.
50. Aimanianda V, Bayry J, Bozza S, Kniemeyer O, Perruccio K, Elluru SR, Clavaud C, Paris S, Brakhage AA, Kaveri SV, Romani L, Latge JP. 2009. Surface hydrophobin prevents immune recognition of airborne fungal spores. Nature 460:1117–1121. https://doi.org/10.1038/nature08264.
51. Bruder Nascimento AC, Dos Reis TF, de Castro PA, Hori JI, Bom VL, de Assis LJ, Ramalho LN, Rocha MC, Malavazi I, Brown NA, Valiante V, Brakhage AA, Hagiwara D, Goldman GH. 2016. Mitogen-activated protein kinases $SakA^{HOG1}$ and MpkC collaborate for *Aspergillus fumigatus* virulence. Mol Microbiol 100:841–859. https://doi.org/10.1111/mmi.13354.
52. Livak KJ, Schmittgen TD. 2001. Analysis of relative gene expression data using real-time quantitative PCR and the $2^{-\Delta\Delta CT}$ method. Methods 25:402–408. https://doi.org/10.1006/meth.2001.1262.
53. Damveld RA, Arentshorst M, Franken A, vanKuyk PA, Klis FM, van den Hondel CA, Ram AF. 2005. The *Aspergillus niger* MADS-box transcription factor RlmA is required for cell wall reinforcement in response to cell wall stress. Mol Microbiol 58:305–319. https://doi.org/10.1111/j.1365-2958.2005.04827.x.
54. Weirauch MT, Yang A, Albu M, Cote AG, Montenegro-Montero A, Drewe P, Najafabadi HS, Lambert SA, Mann I, Cook K, Zheng H, Goity A, van Bakel H, Lozano JC, Galli M, Lewsey MG, Huang E, Mukherjee T, Chen X, Reece-Hoyes JS, Govindarajan S, Shaulsky G, Walhout AJM, Bouget FY, Ratsch G, Larrondo LF, Ecker JR, Hughes TR. 2014. Determination and inference of eukaryotic transcription factor sequence specificity. Cell 158:1431–1443. https://doi.org/10.1016/j.cell.2014.08.009.
55. Chung D, Barker BM, Carey CC, Merriman B, Werner ER, Lechner BE, Dhingra S, Cheng C, Xu W, Blosser SJ, Morohashi K, Mazurie A, Mitchell TK, Haas H, Mitchell AP, Cramer RA. 2014. ChIP-seq and *in*

vivo transcriptome analyses of the *Aspergillus fumigatus* SREBP SrbA reveals a new regulator of the fungal hypoxia response and virulence. PLoS Pathog 10:e1004487. https://doi.org/10.1371/journal.ppat.1004487.
56. Hartree EF. 1972. Determination of protein: a modification of the Lowry method that gives a linear photometric response. Anal Biochem 48:422–427. https://doi.org/10.1016/0003-2697(72)90094-2.
57. Caster SZ, Castillo K, Sachs MS, Bell-Pedersen D. 2016. Circadian clock regulation of mRNA translation through eukaryotic elongation factor eEF-2. Proc Natl Acad Sci U S A 113:9605–9610. https://doi.org/10.1073/pnas.1525268113.
58. Bayram O, Bayram OS, Valerius O, Johnk B, Braus GH. 2012. Identification of protein complexes from filamentous fungi with tandem affinity purification. Methods Mol Biol 944:191–205. https://doi.org/10.1007/978-1-62703-122-6_14.
59. Manfiolli AO, de Castro PA, Dos Reis TF, Dolan S, Doyle S, Jones G, Riano Pachon DM, Ulas M, Noble LM, Mattern DJ, Brakhage AA, Valiante V, Silva-Rocha R, Bayram O, Goldman GH. 2017. *Aspergillus fumigatus* protein phosphatase PpzA is involved in iron assimilation, secondary metabolite production, and virulence. Cell Microbiol 19:e12770. https://doi.org/10.1111/cmi.12770.
60. da Silva Ferreira ME, Kress MR, Savoldi M, Goldman MH, Hartl A, Heinekamp T, Brakhage AA, Goldman GH. 2006. The *akuB*^{KU80} mutant deficient for nonhomologous end joining is a powerful tool for analyzing pathogenicity in *Aspergillus fumigatus*. Eukaryot Cell 5:207–211. https://doi.org/10.1128/EC.5.1.207-211.2006.